SAND99-0068C

# APPLICATION OF ELECTRON BACKSCATTERED DIFFRACTION (EBSD) AND ATOMIC FORCE MICROSCOPY (AFM) TO DETERMINE TEXTURE, MESOTEXTURE, AND GRAIN BOUNDARY ENERGIES IN CERAMICS

RECEIVED
JUN 09 1999
OSTI

S.J. GLASS and V.R. VEDULA
Sandia National Laboratories, Albuquerque, NM, USA
D.M. SAYLOR and G.S. ROHRER
Carnegie Mellon University, Pittsburgh, PA, USA

## Abstract

Crystallographic orientations in alumina ($Al_2O_3$) and magnesium aluminate spinel ($MgAl_2O_4$) were obtained using electron backscattered diffraction (EBSD) patterns. The texture and mesotexture (grain boundary misorientations) were random and no special boundaries were observed. The relative grain boundary energies were determined by thermal groove geometries using atomic force microscopy (AFM) to identify relationships between the grain boundary energies and misorientations.

Keywords: Ceramic, texture, grain boundary energies, EBSD, AFM

## 1 Introduction

The microstructural evolution of materials and their properties (electrical, superconducting, optical, mechanical, thermal) depend on several factors, including the surface and grain boundary energies, orientations, and chemistry. These quantities are interdependent and the complexity of the relationships represents a serious challenge. There is mounting evidence that texture and the presence of special boundaries dominate overall material behavior (Lehockey et al. 1998).

We are interested in crack propagation in polycrystalline ceramics, in particular the influence of residual stresses that develop on cooling from the processing temperature due to thermal expansion anisotropy (see Vedula 1999). If high energy boundaries are preferentially eliminated during microstructural evolution, this may lead to a microstructure that has more fracture resistant boundaries (Gell 1967). The removal of certain misorientations may also influence the residual stresses and the onset of microcracking because textured microstructures with preferred orientations will have more small angle boundaries (Goyal 1996).

## DISCLAIMER

Portions of this document may be illegible in electronic image products. Images are produced from the best available original document.

While relationships between grain size, shape, and material properties have been extensively studied, until the advent of the collection of electron backscattered diffraction (EBSD) patterns, it was not possible to characterize both the texture (lattice orientations) and mesotexture (grain boundary misorientations) and to relate them to the microstructure for a sufficient number of grains to be representative of a real material. There have been few studies on ceramics such as $Al_2O_3$.(Glass et al. 1998 and Mulvihill et al. 1998) It has also not been possible to determine grain misorientations/grain boundary energy relationships.

Our objective is to determine the texture and mesotexture of polycrystalline $Al_2O_3$ and $MgAl_2O_4$ using EBSD and to determine if and how the misorientations relate to the relative grain boundary energies. The measurements of these quantities are a starting point for structure/property simulations (see paper by Vedula) and are also useful for the validation of models of microstructural evolution that incorporate grain boundary energies and grain misorientations. In the present work, the grain boundary energy is assumed to be a function only of its misorientation.

## 2 Experimental procedure

### 2.1 Materials

The polycrystalline ceramic materials used in this study were a 99.99% pure alumina (AKP-50, Sumitomo Chemical Company) and $MgAl_2O_4$ (RCS Technologies). The complete description of the preparation of the alumina can be found elsewhere (Kovar and Readey 1994). Quantitative stereology provided mean grain sizes ($d_{avg}$) of 8 and 27 μm for the 99.99% alumina and the grain shape is close to equiaxed. Densities ranged from 98.6% theoretical density (TD) for the fine-grained material to 99.2% TD for the coarse grained $Al_2O_3$.

### 2.2 Sample preparation

After sintering, the samples were ground and polished flat and parallel with a diamond suspension. The final polishing step for the 27 μm $Al_2O_3$ used colloidal silica (pH=10), whereas for the 8 μm $Al_2O_3$, it was 0.25 μm diamond. The final polishing step for $MgAl_2O_4$ used colloidal silica (pH=7). The grain boundaries were thermally grooved in air at 1600°C for 1 and 100 hr for the 8 and 27 μm grain size samples respectively. The $MgAl_2O_4$ was thermally etched at 1500°C for 10 hr.

### 2.3 Atomic force microscopy (AFM) measurements

Surface dihedral angles were measured for the thermal grain boundary grooves on the samples using a Digital Instruments StandAlone AFM (SAA-125) positioned above the sample mounted on an X-Y translation stage (Burleigh Instruments TSE-150) with reproducible position resolution of 50 nm. Details about the imaging and error minimization can be found elsewhere (Saylor and Rohrer 1998). For the alumina and spinel samples respectively, 164 and 175 three-grain junctions were measured. The grain boundary to surface energy ratios were obtained from the simplified Herring equation $\gamma_{gb}/\gamma_s=2\cos(\psi/2)$ that assumes the torque terms are zero, the surface energies are isotropic and the grain boundary energy is a function of misorientation only.

## 2.4 Electron Backscattered Diffraction (EBSD) pattern collection

EBSD were collected using a Phillips SL40FEG scanning electron microscope (SEM). The same grains examined by AFM were located using fiducial marks and EBSD were obtained for each of the manually selected grains. The patterns were indexed using TSL's Orientation Imaging Microscopy Software (TexSEM Labs, Inc.) assuming cubic symmetry for spinel and hexagonal symmetry for alumina. Orientations were specified by a set of Euler angles ($\alpha$, $\beta$, $\gamma$) for each grain that defines a rotation matrix with respect to the specimen coordinate system. Misorientations were defined using the Euler angles from adjoining grains and deriving the pair's common axis and the rotation angle about that axis that brings the crystallites into coincidence (so-called axis/angle pairs). The smallest positive misorientation angle from the misorientation matrix was used.

# 3 Results and Discussion

## 3.1 Surface Energies from AFM Measurements

The cumulative probability distribution of dihedral angles along with the grain boundary energy ratios is shown in Fig. 1. The mean value of the dihedral angle for the 8 μm alumina distribution and the corresponding value of $\gamma_{gb}/\gamma_s = 0.95$ are similar to those obtained for another alumina (1.1 to 1.2) using a metal reference line technique; however, the distribution is wider (Handwerker, 1990).

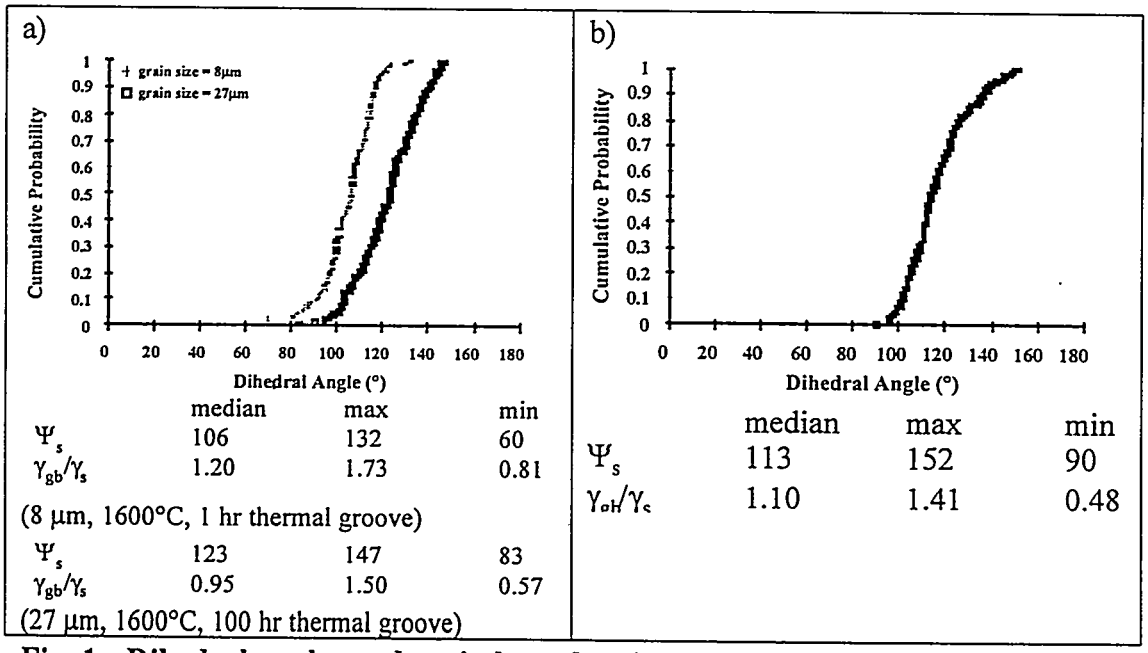


a)

| | median | max | min |
|---|---|---|---|
| $\Psi_s$ | 106 | 132 | 60 |
| $\gamma_{gb}/\gamma_s$ | 1.20 | 1.73 | 0.81 |
| (8 μm, 1600°C, 1 hr thermal groove) | | | |
| $\Psi_s$ | 123 | 147 | 83 |
| $\gamma_{gb}/\gamma_s$ | 0.95 | 1.50 | 0.57 |
| (27 μm, 1600°C, 100 hr thermal groove) | | | |

b)

| | median | max | min |
|---|---|---|---|
| $\Psi_s$ | 113 | 152 | 90 |
| $\gamma_{oH}/\gamma_c$ | 1.10 | 1.41 | 0.48 |

**Fig. 1: Dihedral angles and grain boundary/surface energy ratios for a) 8 and 27 μm alumina etched at 1600°C for 1 and 100 hr. respectively. b) $MgAl_2O_4$.**

The higher mean dihedral angle and lower mean ratio of $\gamma_{gb}/\gamma_s$=1.20 for the 27 μm alumina compared to the 8 μm sample and Handwerker's results for a 99.99% pure alumina may be a result of differences in sample processing, grain size, and the

difference in the surface preparation technique. The diamond polish produces more damage and may change the energies and diffusivities in the system. There is also the possibility that the colloidal silica contaminates the grain boundaries. The values for $MgAl_2O_4$ are within the range of values tabulated by Handwerker for other ceramics.

### 3.2 Grain Boundary Misorientations

The grain boundary misorientations and their relationships to the $\gamma_{gb}/\gamma_s$ ratio are shown in Fig. 2 for both $Al_2O_3$'s and the $MgAl_2O_4$. There are no low angle boundaries for either the 27 μm $Al_2O_3$ or $MgAl_2O_4$ samples. None of the measured boundaries are CSL boundaries with respect to Brandon's criterion. There is no clustering of the orientations and there is no apparent correlation between the misorientation and the $\gamma_{gb}/\gamma_s$ ratio. Similar results were found for the $MgAl_2O_4$. The absence of special boundaries and a relationship between the energy and misorientation of some boundaries is in contrast to results for a MgO sample (Saylor and Rohrer 1998). Although both materials in this study have relatively high purities, the presence of glass and other grain boundary impurities may be important (Swiatnicki 1995). The grain boundary plane and atomic level faceting along the boundary may play large roles in determining the grain boundary energies, although random grain boundaries generally have higher energy and are less sensitive to the orientation of their grain boundary planes (Garbacz 1995). A TEM study of grain boundaries in alumina showed more near coincidence grain boundaries in a small grain sized homogeneous microstructure with no dense interfacial planes than in one containing abnormally large grains with boundaries with densely packed planes (Swiatnicki 1995). The materials in this study are relatively large grained.

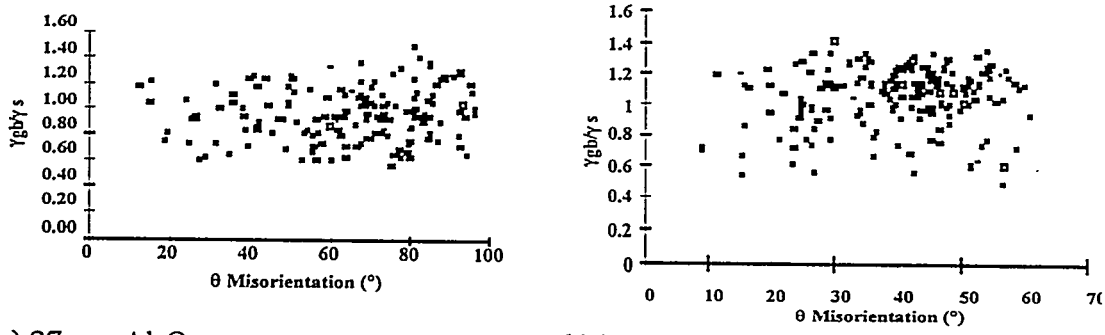


a) 27 μm $Al_2O_3$ b) $MgAl_2O_4$

**Fig. 2: Grain boundary energy ratio vs. misorientation angle (θ).**

### 3.3 Texture

The pole figure for the 27 μm alumina is shown in Fig. 3, where RD and TD represent the two directions parallel to the specimen axes. Each of the points represents a grain in the polycrystal for which the grain boundary energy ratios were measured. Based on these measurements and measurements for similar materials the alumina has random texture. Even in alumina materials that have been hot pressed to introduce texture,(Ma 1991) only small degrees of texture have been observed relative

to the texture observed in many metal systems. In other materials systems it has been shown that the presence of grain texture has a significant effect on the grain misorientation textures (Randle 1988). Thus the absence of misorientation texture is consistent with the absence of grain texture.

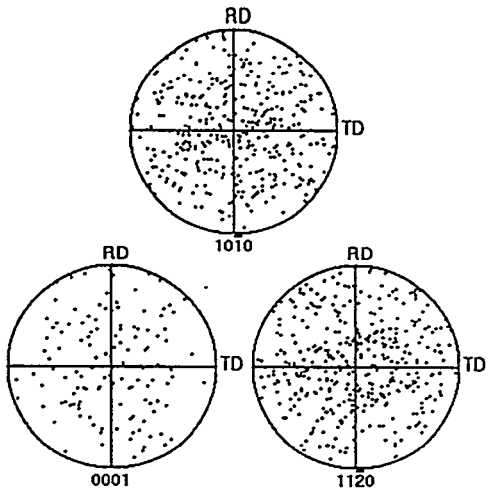


**Fig. 3: Pole figures for 27 μm alumina.**

## 4 Summary and Conclusions

Mean grain boundary to surface energy ratios were in the range of one for alumina and spinel. The differences for the two grain sizes of alumina need to be resolved to determine if they are due to intrinsic differences in the grain boundary energy distribution for different grain sizes or due to surface preparation techniques. The samples examined in this study have random texture and random misorientations and do not contain CSL boundaries. Ceramic materials that are expected to have more texture should be examined to identify effects and relationships that may be subtle.

**Acknowledgments**

*Sandia is a multiprogram laboratory operated by Sandia Corporation, a Lockheed Martin Company, for the United States Department of Energy under Contract DE-ACO4-94AL85000. This work was supported in part by the MRSEC Program of the National Science Foundation under Award Number DMR-9632556.*

## 5 References

Garbacz, A, Ralph, B, Kurzdylowski, K.J. (1995) On the possible correlation between grain size distribution and distribution of CSL boundaries in polycrystal, *Acta metall. mater.*, Vol. 43, No. 4, pp. 1541-1547.

Gell, M., Smith, E. (1967) The propagation of cracks through grain boundaries in polycrystalline 3% silicon-iron, *Acta met*, Vol. 15, pp. 253-258.

Glass, S.J., Michael, J.R., Readey, M.J., Wright, S.I., Field, D.P., (1998) Characterization of microstructure and crack propagation in alumina using orientation imaging microscopy (OIM), pp. 803-813 in Ceramic Microstructures – Control at the Atomic Level, Edited by A.P. Tomsia and A.M. Glaeser, Plenum Press, NY.

Goyal, A., Specht, E.D., Kroeger, D.M., Mason, T.A. (1996) Effect of texture on grain boundary misorientation distributions in polycrystalline high temperature superconductors, *Appl. Phys. Lett.*, Vol. 68, No. 5, pp. 711-713.

Handwerker, C.A., Dynys, J.M., Cannon, R.M., Coble, R.L. (1990) Dihedral angles in magnesia and alumina: distributions from surface thermal grooves, *J. Am. Ceram. Soc.*, Vol. 73, No. 5, pp. 1371-77.

Kovar, D., Readey, M.J. (1994) Role of grain size in strength variability of alumina, *J. Am. Ceram. Soc.* 77:1928-38.

Lehockey, E.M., Palumbo, G., Lin, P. (1998) Improving the weldability and service performance of nickel- and iron-based superalloys by grain boundary engineering *Meta. Mat. Trans A-Phy. Meta. Mat. Sc.* 29[12] pp. 3069-3079.

Ma, Y, Bowman, K.J. (1991) Texture in hot-pressed or forged alumina, *J. Am. Ceram. Soc.*, Vol. 74, No. 11, pp. 2941-44.

Mulvihill, M.L., Gülgün, M.A., Bischoff, E., Rühle, M (1998) Orientation imaging microscopy of alpha alumina: sample preparation and texture analysis, *Z. Metallkd.*, Vol. 89, No. 8, pp. 546-550.

Randle, V., Ralph, B., Dingley, D. (1988) The relationship between microtexture and grain boundary parameters, *Acta metall.*, Vol. 36, No. 2, pp. 267-273.

Saylor, D.M. and Rohrer, G.S. (1998) Measuring the influence of grain boundary misorientation on thermal groove geometry in ceramic polycrystals. Submitted to *J. Am. Ceram. Soc.*

Swiatnicki, W., Lartigue-Korinek, S., Laval, J.Y. (1995) Grain boundary structure and intergranular segregation in alumina, *Acta metall. mater.*, Vol. 43, No. 2, pp. 795-805.

Vedula, V.R., Glass, S.J., Saylor, D.M., Rohrer, G.S., Carter, W.C., (1999) Predicting microstructural-level stresses and crack paths in ceramics, *ICOTOM-12* (1999).